Marine Geology 399 (2018) 84–96

Contents lists available at ScienceDirect

Marine Geology

journal homepage: www.elsevier.com/locate/margo

Large sediment waves over the Gulf of Roses upper continental slope (NW Mediterranean)

Marta Ribó[a,b,*], Ruth Durán[a], Pere Puig[a], David Van Rooij[c], Jorge Guillén[a], Pere Masqué[d,e,f]

[a] Marine Sciences Institute, Consejo Superior de Investigaciones Científicas (ICM-CSIC), Marine Geosciences Department, Barcelona, 08003, Spain
[b] Marine Climate Risk Group, Department of Environmental Science, Macquarie University, Sydney, Australia
[c] Ghent University, Department of Geology and Soil Science, Renard Centre of Marine Geology, Krijgslaan 281 s8, B-9000 Ghent, Belgium
[d] Departament de Física & Institut de Ciència i Tecnologia Ambientals, Universitat Autònoma de Barcelona, Bellaterra, Spain
[e] Oceans Institute and School of Physics, University of Western Australia, Crawley, WA, Australia
[f] School of Science, Edith Cowan University, Joondalup, WA, Australia

ARTICLE INFO

Keywords:
Sediment waves
Continental slope
NW Mediterranean Sea
Dense shelf water cascading (DSWC)

ABSTRACT

Large sediment waves have been observed over the Gulf of Roses (GoR) continental slope (NW Mediterranean), developed between ~200 and ~400 m water depth. Geometric parameters computed from the acquired swath bathymetry revealed mean wave lengths of ~2000 m, and maximum wave heights of ~60 m. Single-channel reflection seismic profiles provided information on the sediment wave internal structure and the Quaternary stratigraphic architecture of the GoR outer shelf and slope. Seven main seismic units could be identified, with continuous development of sediment waves over the outer continental shelf and upper slope, showing differences in wave height and length. The seismic units are differentiated by erosional surfaces that can be followed from the outer shelf down the slope, and which have been correlated with Pleistocene eustatic oscillations. Sediment cores were collected over the sediment wave crests and troughs, and grain size distribution and sediment accumulation rates were analysed. Results show a dominant fraction of fine sediments, allowing classifying the observed bedforms as mud waves. Calculated sediment accumulation rates ranged between 0.08 and 0.18 cm/y, with no clear sedimentation pattern (e.g. differential sediment deposition rates) observed between wave crests and troughs. Nevertheless, the presence of thick surface mixed layers and the increase of the sand fraction in the upper sections of the cores indicate that the surface sediments are affected by bottom trawling activities, since the area is highly impacted by this human activity. The sediment waves observed over the GoR slope are most likely to be formed by bottom currents generated by overflows of dense water originated in the Gulf of Lions shelf, which cascade downslope in an oblique angle with respect the main bathymetric contours. This study offers new insights on the role of dense shelf water cascading processes and associated off-shelf sediment transport reshaping the morphology of the open-slope regions.

1. Introduction

Sediment waves, defined as large-scale depositional bedforms, can display a wide range of morphologies, dimensions and sediment types (i.e., gravel-, sand- and mudwaves). These features have been observed worldwide in a variety of environments and water depths, generated by sediment transport processes on the bottom boundary layer, such as bottom currents (i.e., alongslope-flowing bottom currents) (Mosher and Thomson, 2002; Masson et al., 2002), turbidity currents (i.e., downslope-flowing turbidity currents) (Wynn et al., 2000; Lee et al., 2002), mixed origin (differential sediment depositional over a pre-existing complex seafloor topography, derived from initial sediment deformation) (Faugères et al., 2002; Cattaneo et al., 2004), or the interaction of internal waves with the seabed over the sloping seafloor (Reeder et al., 2011; Delivet et al., 2016; Ribó et al., 2016a, 2016b). Moreover, downslope bottom currents enhanced by dense shelf waters (DSW) have been also reported to be a mechanism for the formation of sediment waves in upper continental slope areas (Verdicchio and Trincardi, 2006; Anderskouv et al., 2010; Foglini et al., 2016).

The formation of DSWs occur in wide and large shelf regions, when the density of the water in the inner shelf increases, due to an increase in salinity (caused by evaporation or ice formation) and/or a decrease in temperature through cooling (Ivanov et al., 2004). These dense waters can be transported across-shelf, cascading down the continental slope to greater depths, as a near bed gravity current with entrained sediments sinking down to its compensation level (Fieux, 1974; Wilson

* Corresponding author.
E-mail address: marta.ribogene@mq.edu.au (M. Ribó).

https://doi.org/10.1016/j.margeo.2018.02.006
Received 28 September 2017; Received in revised form 7 February 2018; Accepted 11 February 2018
Available online 15 February 2018
0025-3227/

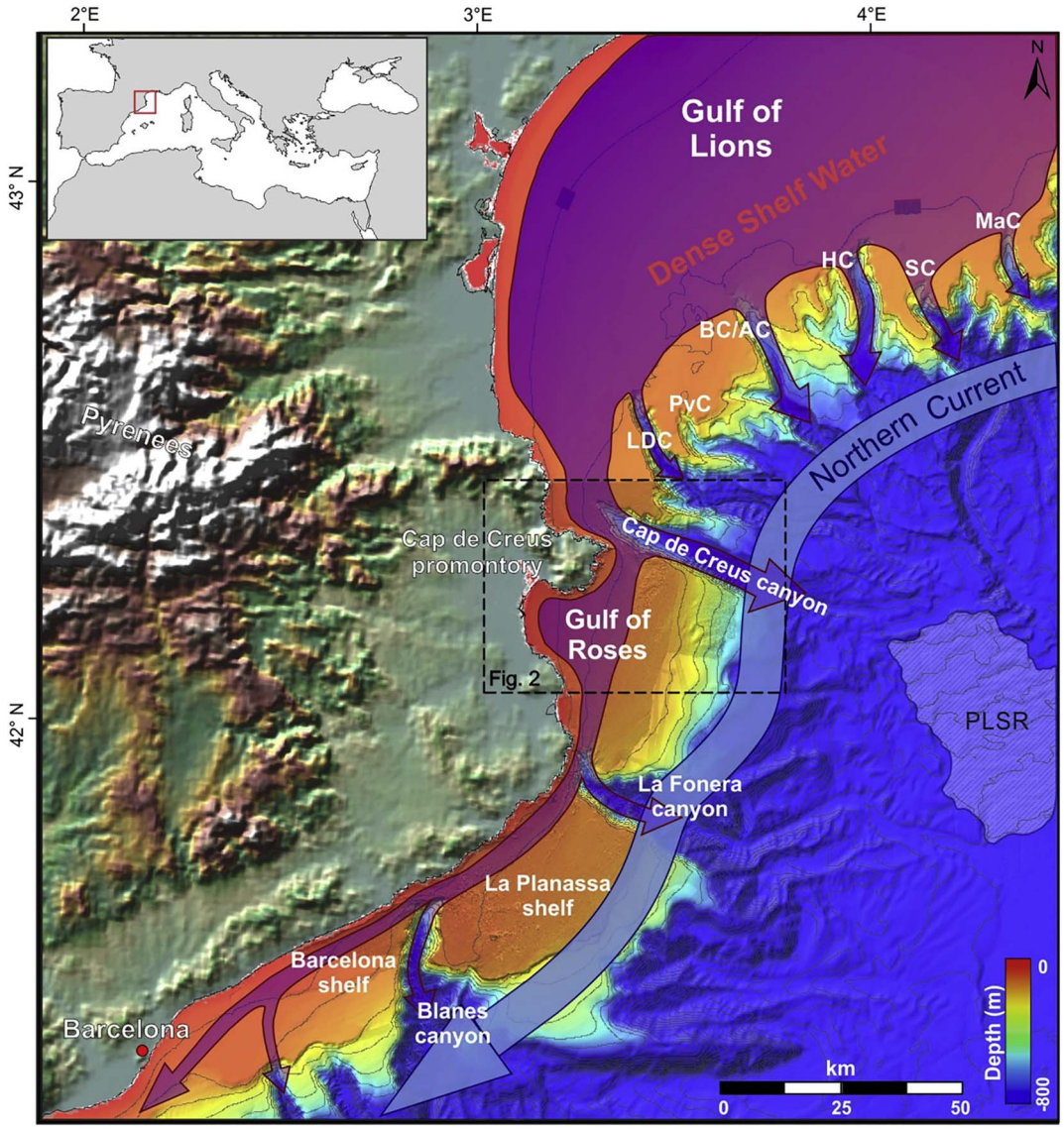

Fig. 1. Location map and bathymetry of the North Catalan margin from the Gulf of Lions (GoL) to the Gulf of Roses (GoR), showing along-slope Northern Current circulation, the major dense shelf water formation and off-shelf export through the submarine canyons, and the location of the Pyreneo-Languedocian Sedimentary Ridge (PLSR). LDC: Lacaze-Duthiers Canyon; PvC: Pruvot Canyon; B/AC:Bourcart or Aude Canyon; HC: Herault Canyon; SC: Séte Canyon; MaC: Marti Canyon. Dashed line box indicates the location of Fig. 2. Multibeam mosaic is a composition of the data from GEBO Digital Atlas (IOC et al., 2003) and the Catalano-Balearic Sea bathymetric chart build from several oceanographic surveys (Farrán, 2005).

and Roberts, 1995; Shapiro et al., 2003; Durrieu de Madron et al., 2005). The dense shelf water cascading (DSWC) events can last for several weeks, with strong currents that can induce erosion and resuspension of sediments in the outer shelf and upper slope (Fohrmann et al., 1998). Sediment transport and seafloor shaping resulting from the bottom currents enhanced by DSWC events on the Gulf of Lions (GoL) and the northern Catalan margin (Fig. 1) have been widely described (Canals et al., 2006; Palanques et al., 2006, 2008; Lastras et al., 2007, 2011; Puig et al., 2008; Durán et al., 2014, among others). However, most of the studies have mainly focussed on the sediment processes within the submarine canyon and/or over shelf areas, whereas their impact on the open slope and basin has received less attention and is still poorly known (Jallet and Giresse, 2005; Palanques et al., 2011, 2012; Puig et al., 2013). New evidences of sediment transfer across the Gulf of Roses (GoR) continental slope are here provided, in agreement with the hydrodynamic DSWC downslope pathways. This study aims to characterize the morphology and internal structure of the GoR upper continental slope, where the occurrence of sediment waves is observed, previously related to slump and creep-like deformation (Ercilla et al., 1994). New detailed bathymetric, seismic and geochronology data allowed a new interpretation of the observed sediment waves and their formation processes. This paper will contribute to a better understanding of the sedimentary evolution of the Northern Catalan margin and how the sediment deposition and accumulation can be disrupted by human activities such as bottom trawling.

1.1. Regional setting

1.1.1. Geological and morphological setting

The GoR extends over an area of ~1000 km^2 south from the Cap de Creus promontory, on the Northern Catalan margin, NW Mediterranean (Fig. 1). The pre-Cenozoic basement structure of this margin is defined by NW-SE to NNW-SSE normal faults, which originated a system of horsts and grabens reflected in the present-day configuration of the coastal plain (Muñoz et al., 1986; Maillard et al., 1992; Tassone et al., 1996; Ercilla et al., 1994; Roca et al., 1999; García et al., 2011). The pre-Messinian sedimentary record in the Catalan margin includes Lower to Upper Oligocene sediments deposited in piggyback basins during the pre-extensional episode; Lower Miocene sediments deposited in the graben troughs during the *syn*-rift episode; and late Langhian to

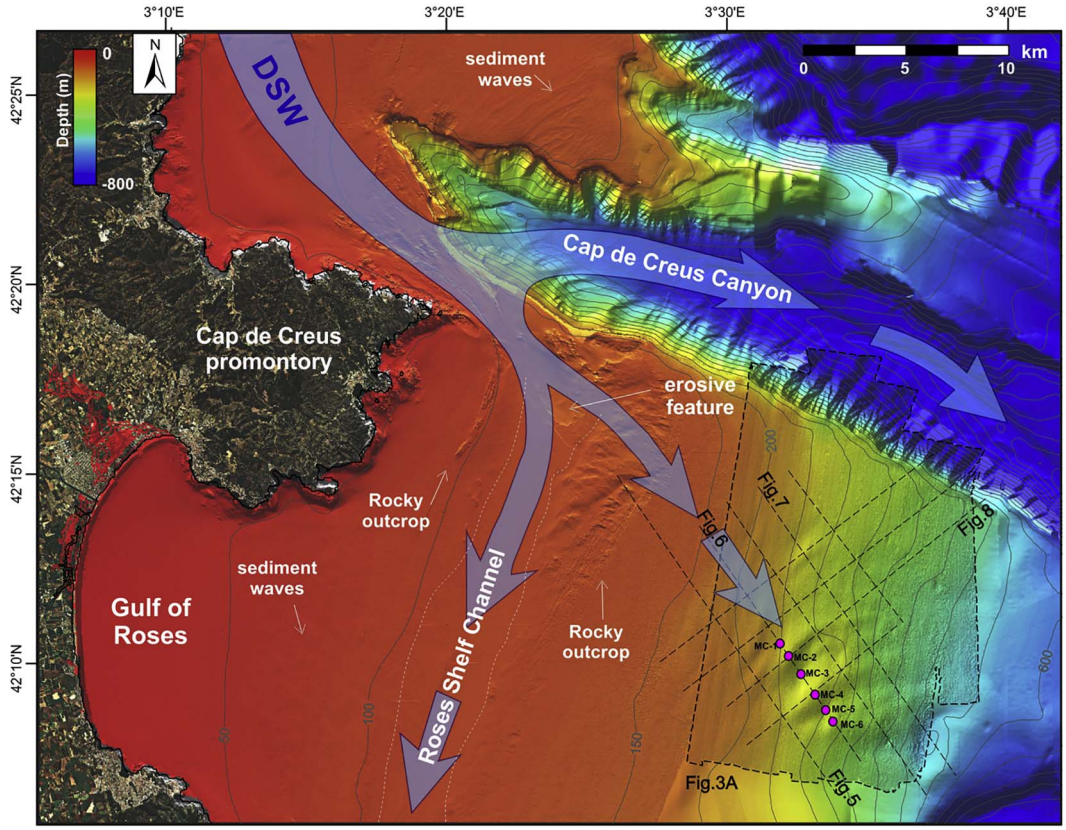

Fig. 2. Bathymetric map of the southern part of the Gulf of Lions, including the Cap de Creus submarine canyon, and the Gulf of Roses (GoR) continental shelf and upper slope. Black dashed line indicates the coverage of the recently acquired swath bathymetry. Blue arrows indicate the deep shelf water (DSW) circulation through the Cap de Creus canyon and towards the GoR (smaller arrows). The major morphological features observed over the continental shelf are indicated, as well as the location of the multicore (MC) sediment samples collected (pink dots numbered from MC-1 to MC-6), the location of the acquired single-channel seismic profiles (dashed lines) and the profiles shown in Figs. 4, 5, 6 and 7. Modified from Ribó et al. (2017). (For interpretation of the references to colour in this figure legend, the reader is referred to the web version of this article.)

Messinian sequences showing a gradual transition to the post-rift stage (Roca et al., 1999). The Pleistocene sedimentation over the GoR continental shelf was controlled by high-frequency sea level changes, which originated a progressive downwarping of the sedimentary deposits, and the apparent flexuring of these deposits towards the continental slope (Got, 1973; Stanley et al., 1976). Overall, the Plio-Quaternary sedimentary pattern has been defined by vertically stacked seaward-downlapping regressive deposits, building a progradational growth pattern, mainly controlled by high-frequency eustatic sea-level changes (Ercilla et al., 1994).

The GoR continental shelf width varies from ~2.6 km near the Cap de Creus Canyon to ~30 km wide in the centre of the gulf (Fig. 2). The shelf gradient ranges from 0.4° to 0.6°, and shelf edge is located approximately at 150 m water depth. Three subareas have been defined in the continental shelf based on physiographic characteristics: inner shelf (0–60 m water depth), middle shelf (60–90 m water depth) and outer shelf (> 90 m water depth) (Durán et al., 2014). The outer shelf is characterized by the presence of a 1.5 km wide, 15 m deep channel-like depression, at ~125 m water depth (Lastras et al., 2011). This structure, known as the Roses Shelf Channel, is oriented NNE-SSW and it extends for 40 km along the GoR shelf from the southern rim of the Cap de Creus submarine canyon upper course (Fig. 2). This erosive shelf channel has its inner and outer shoulders consisting of rocky alignments parallel to the shelf edge (Lastras et al., 2011; Durán et al., 2014), covered by coarse sediments (Lo Iacono et al., 2010). Numerous rocky outcrops are observed on the middle and outer continental shelf, and north of the Cap de Creus promontory (Fig. 2). Normal faulting affecting the study area was suggested to control the rocky outcrops and the shelf edge location, and could also have influenced the inception of the Roses Shelf Channel (Muñoz et al., 1986; Maillard et al., 1992; Roca et al., 1999; Durán et al., 2014).

Several erosive features, such as lineations, elongate and oval depressions and obstacle marks have been identified over the GoR continental shelf (Durán et al., 2014). Moreover, a field of elongated sediment waves has been observed on the mid-outer shelf (Fig. 2), in between 50 and 100 m water depth, oblique to the bathymetric contours (Urgeles et al., 2011; Durán et al., 2014). It has been suggested that the observed erosive and depositional features are the result of strong bottom currents (~50 cm s^{-1}), apparently related with the advection of dense shelf waters and/or induced by large wind storms and/or the general geostrophic circulation (Ogston et al., 2008; Durán et al., 2014).

In deeper waters, a thick sedimentary body, named the Pyreneo-Languedocian Sedimentary Ridge (PLSR; Fig. 1), was identified at the base of the continental slope by Berné and Loubrieu (1999) during the CALMAR cruise in 1997. The PLSR is characterized by the presence of sediment waves, which were initially interpreted as creep-folds (Canals-Artigas, 1985). Such sediment waves were re-interpreted by Jallet and Giresse (2005) to be related to turbidite or a gravity-flow overspill from the Cap de Creus Canyon and the Sète Valley. Seven relict sets (units) of sediment waves were observed by the authors, corresponding to periods of important terrigenous supplies linked to major low-stand intervals. The sediment supplied from the shelf or the upper slope was suggested to be responsible for part of the overflows that travelled across the PLSR, representing a continuous background of sediment deposition, interrupted by intervals of ambient hemipelagic sedimentation, generating the wave fields over hundreds of thousands of years (main part of the Quaternary).

1.1.2. Hydrodynamics and sediment processes settings

The GoR is located in the Northern Catalan margin, where the general circulation exhibits a seasonal variability with significant spatial mesoscale fluctuations, playing a decisive role in exchange process between shelf and oceanic waters (La Violette et al., 1990; Font et al., 1995). This area is characterized by the geostrophic Northern Current, which forms a 30-km wide meandering jet flowing southwestward along the upper continental slope (Fig. 1), with maximum speeds of up to 50 cm s^{-1} (Durrieu de Madron et al., 1990; Font et al., 1995; Millot, 1999; Flexas et al., 2002).

The GoR continental shelf currents are dominated by storms mainly coming from the E (Mendoza et al., 2011), but can also be affected by the strong and persistent winds coming from the N-NW. During wintertime, these dry and cold winds favour the cooling and homogenization of the continental shelf waters, triggering the formation of the DSWs, primarily in the GoL (Fig. 1) (Béthoux et al., 2002; Durrieu de Madron et al., 2005, 2008; Canals et al., 2006, 2009). The interaction of the storm-induced downwelling and the DSWC events enhances the near-bottom transport of sediment over the continental shelf, advecting resuspended sediments down to greater depths (Palanques et al., 2006, 2008, 2012; Puig et al., 2008). Observations in this area revealed that most of the transport of water and suspended particles occurs through the westernmost submarine canyons in the GoL (Fig. 1), being the Cap de Creus canyon the major sediment transport conduit in the NW Mediterranean Sea during the high-energetic storms and DSWC events (Palanques et al., 2006, 2008; Ulses et al., 2008a, 2008b, 2008c). However, part of the DSW and the associated bottom currents advecting suspended sediment keeps flowing southwards, towards the GoR, channelized between the Cap de Creus promontory and the submarine canyon flank (Fig. 2) (Palanques et al., 2008; DeGeest et al., 2008; Ulses et al., 2008a; Lastras et al., 2011; Ribó et al., 2011). As for the GoR shelf, it has also been identified as an area that contributes to the formation of dense shelf waters, but in smaller quantities (Ulses et al., 2008a; Ribó et al., 2011). Additionally, the GoR continental shelf and slope is highly affected by commercial and fishing activities (Fig. 3B), which might cause surface sediment reworking and resuspension. On the Catalan margin, in regions slightly south of the GoR, it has been observed that ploughing of the seafloor by bottom trawling can trigger sediment gravity flows (Palanques et al., 2006; Martín et al., 2007, 2014); increase downward sediment fluxes and sediment accumulation rates along submarine canyon axes(Martín et al., 2006, 2008;Puig et al., 2015; Paradis et al., 2017), and reshape the continental slope morphology over large spatial scales (Puig et al., 2012).

2. Methods

The results of this study are based on the swath bathymetry acquired in July 2013 during an oceanographic cruise in the frame of the FORMED Project, on board of the R/V García del Cid. The multibeam data was collected using the Elac SeaBeam 1050D 50 kHz multibeam echosounder, and corrected for heading, depth, pitch, heave and roll, and also for the sound speed. Post-processing of the data, including manual cleaning of the spikes (beam removal) and refraction correction, was performed using the CARIS HIPS and SIPS Hydrographic Data Processing System. The processed multibeam surfaces were exported into ASCII format files and imported into ArcGIS Spatial Analyst software to create a Digital Terrain Model (DTM) (20 m grid size) for further analysis. The detailed geo-referenced shaded-relief images were created with sun-illumination with an azimuth of 315° and elevation of 45°, and were three times vertically exaggerated to accentuate the morphologic details. Images are presented using Universal Transverse Mercator (UTM 31 N zone) projection, in the World Geodetic System (WGS 84) geographic coordinate system.

Geometric parameters such as wavelength (spacing between two concurrent waves) and height of each sediment wave, were determined from the bathymetric dataset, extracting bathymetric profiles from the DTM, and using an automated procedure computed by MatLab software.

Eight high-resolution single channel reflection seismic profiles, covering a total length of 150 km, were acquired during the same oceanographic cruise, using a SIG sparker source (120 electrodes). The source was triggered every 3 s with an energy level of 600 J while the vessel velocity was maintained at ~3.5 knots. The seismic profiles were recorded with a surface streamer using a Delph Seismic 2.7.0.0 (Ixsea) acquisition system. Data was pre-filtered using an 80–2000 Hz analogue bandpass filter. The recorded trace length was 2.8 s two-way travel time

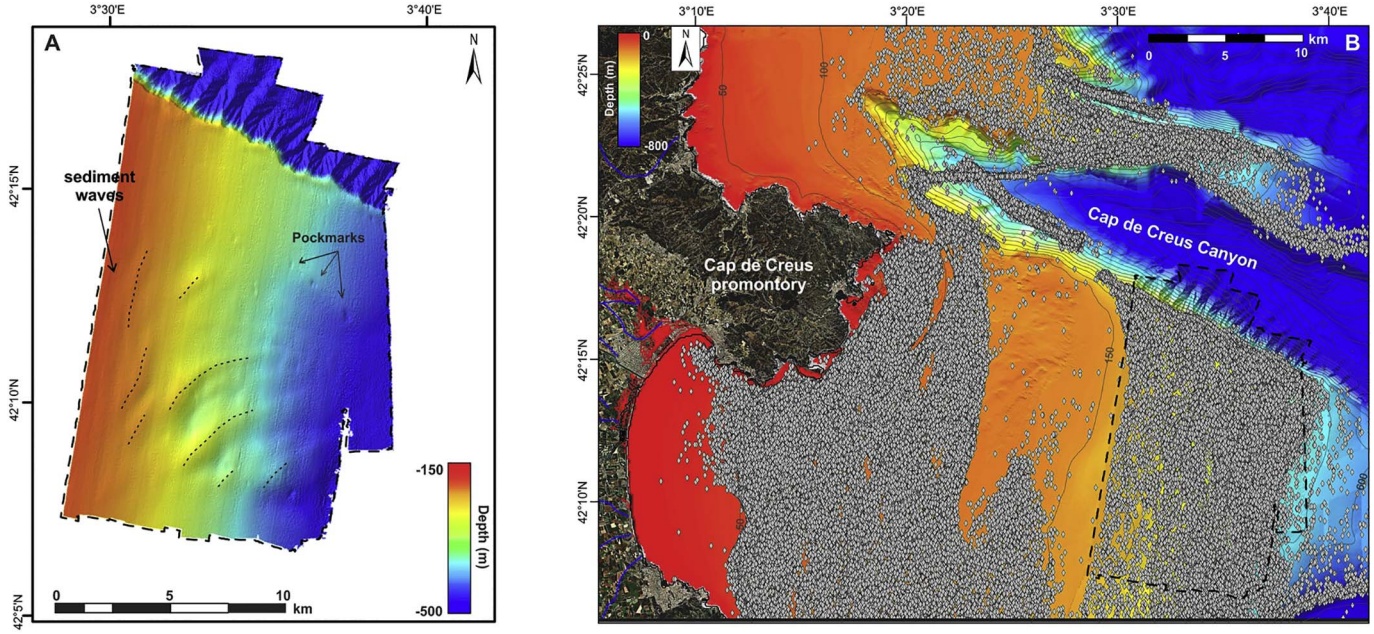

Fig. 3. A) Coloured shaded relief image of the Gulf of Roses outer continental shelf and upper continental slope (20 × 20 m grid) illustrating the sediment waves (dashed lines follow the sediment waves crests) and the pockmarks observed over the continental slope. Modified from Ribó et al. (2017). **B**) Bathymetric map showing the location of the bottom trawl fishing vessels from the Vessel Monitoring System (VMS) information (grey dots). Note that the bottom trawling activity is completely covering the area where the sediment waves field is located.

(TWTT) with a sampling frequency of 10 kHz. The seismic lines were recorded directly in SegY-Motorola format with associated navigation files. Processing of the seismic data (including bandpass filtering, water noise and burst noise removal, amplitude correction, and trace editing) was performed using the seismic processing software RadExPro (Deco Geophysical), while interpretation was performed using the Kingdom Suite software. The mean velocities used for time to depth conversion is 1550 m/s.

Grain size and sedimentation rates over the GoR upper continental slope were determined from six sediment cores collected at water depths in between 245 and 345 m, across the sediment waves (see location in Fig. 2), using a six tube KC-Denmark Multicorer (MC). The sediment cores, with lengths between 41 and 52 cm, were sub-sampled on board immediately after retrieval in slices of 1 cm thick, and stored in sealed plastic bags at −10 °C for later analysis. Dry weights of the sediment samples were determined after lyophilisation in the laboratory, and a representative aliquot of each slice was used for determination of the grain size. Each sample was treated with 20% H_2O_2 and pyrophosphate in order to eliminate the organic matter, and to avoid particle flocculation. After the treatment of the samples, a Horiba LA950 particle size analyser (Horiba Ltd., Kyoto, Japan) was used to determine the distribution of the sediment grain size as volume percentage.

The remaining part of the sample was homogenized in an agate mortar for the analysis of ^{210}Pb to determine the sedimentation rate. This radionuclide, with a half-life of 22.3 years, is an adequate tracer of the sediment accumulation rate (SAR) over periods of up to 100–150 years. The ^{210}Pb analyses were conducted following the method described in Sanchez-Cabeza et al. (1998). Sediment samples of 200–300 g (dry weight) were spiked with a known amount of ^{209}Po as internal tracer and acid-digested using a microwave. The concentration of ^{210}Pb was calculated through the quantification of the activity of its grand-daughter ^{210}Po, assumed to be in equilibrium, by alpha spectrometry. Supported ^{210}Pb (in equilibrium with ^{226}Ra in sediments) was obtained from the constant activity of the deepest samples in each core, confirmed to be in good agreement with ^{226}Ra concentrations of selected samples measured by gamma spectrometry. The difference between total and supported ^{210}Pb determines the excess ^{210}Pb concentrations, used to estimate accumulation rates, using a one-dimensional, steady-state constant ^{210}Pb flux:constant sedimentation model (CF:CS model, Krishnaswamy et al., 1971).

Data from the satellite-based tracking Vessel Monitoring Systems (VMS) of fishing trawlers operating in the GoR was provided by the Fishing Monitoring Centre of the Spanish Secretariat of Maritime Fishing (SEGEMAR). The information provided was encrypted (i.e. without the ship's identification), and consisted on the vessel's position, recorded approximately every 2 h, from 2005 to 2011. This VMS data allowed identifying the areas highly affected by trawling activities nearby the study site.

3. Results

3.1. Gulf of Roses upper slope geomorphology and sedimentology

The newly acquired swath bathymetry, covering an area ~230 km^2 over the GoR slope, revealed the presence of several large sediment waves over the GoR upper continental slope, extending from ~200 m to ~400 m water depth (Figs. 2 and 3A). At this site, the continental slope gradient is relatively gentle, ranging from 1° to 4°, and the sediment waves are very much localised on a specific area, starting below the shelf edge (> 150 m) and tending to disappear at mid-continental slope (~400 m), coinciding where the regional bathymetry orientation changes slightly towards the southeast and the continental slope gradient becomes steeper (> 4°). The orientation of the sediment waves slightly changes from NNE-SSW, at the uppermost part of the slope where the crests are parallel to the regional slope, to a NE-SE orientation, with the sediment wave crests becoming oblique to the regional bathymetric contours (Figs. 2 and 3A). Detailed analysis of the multibeam dataset show several pockmarks north from the sediment wave field, increasing in size downslope, with diameters from 150 to 300 m, and depths from 3 m to 5 m (Fig. 3A). The results of the morphobathymetric analysis showed sediment waves with a maximum lateral continuity up to 3000 m (Fig. 3A). These features are morphologically asymmetrical, with the shorter flank dipping landwards towards the NW, and the longer and steeper (> 5°) flank dipping seawards towards the SE. Geometric parameters were analysed from bathymetric profiles (perpendicular to the sediment wave crests) and the obtained results revealed mean wave lengths of ~2000 m and maximum wave heights of ~60 m.

It is observed that the GoR continental shelf and slope is highly affected by bottom trawling fishing (Fig. 3B). This area is harvested by the Roses harbour fishing fleet, and trawling grounds occupy the entire upper continental slope down to 800 m water depth. Although the area is highly impacted by such human activities, surface sediments over the sediment waves are consistently uniform, with dominant silt (up to ~60–70%) and clay (~25%), and a small portion (~5–15%) of sand. The grain size analysis results show that the observed bedforms are fine-grained sediment waves or mud waves, following the classification from Wynn and Stow (2002). However, it should be pointed out that the cores collected over the crest (MC 2 and 4) showed higher sand fraction on the upper 10 cm than the cores collected on the troughs (MC 3 and 5) (Fig. 4). In addition to that, it is worth noting that there is an increase of the sand portion on the upper 5–10 cm of the sediment cores (Fig. 4).

Sediment accumulation rates (SARs) were calculated from the samples taken on the crests (MC 2, 4 and 6) and on troughs (MC 1, 3 and 5) of two adjacent sediment waves (see location in Fig. 2). The distribution of excess ^{210}Pb in a sediment core, under steady conditions of sediment accumulation and bioturbation, usually differentiates in two zones: a surface mixed layer (SML), where bioturbation or physical mechanisms mix the sediment producing a layer of uniform concentration of the excess of ^{210}Pb; and a layer of exponential decrease of the excess of ^{210}Pb activity (Fig. 4). The apparent accumulation rates can be estimated from the slope of the log-linear fit of the decreasing excess of ^{210}Pb in each sediment core versus the accumulated mass (Nittrouer et al., 1984; Masqué et al., 2002). In the study site the SML extends down to core depths between 10 and 15 cm, and is evident in almost all the sediment cores, except for MC-6 (Fig. 4). Values of ~100 Bq/kg are typically found on the surface within the SML, but MC-6 shows these values on the layer of exponential decrease of the excess of ^{210}Pb activity, and the SML is missing (Fig. 4). Overall, SARs calculated on the multicores showed values ranging between 0.08 and 0.18 cm/y (i.e., between 0.07 and 0.14 g·cm^{-2}·y^{-1}), with no clear differential sediment deposition rates being identified between sediment wave crests and troughs (Fig. 4).

3.2. Seismic stratigraphy of the Gulf of Roses continental slope

The internal structure of the sediment waves was determined from the single-channel seismic profiles acquired over the GoR outer shelf and slope (see location on Fig. 2). Seven main units are differentiated (see Table 1), and sediment waves are identified, with a clear up-slope migrating pattern and varying in wave height and length within the different units (see Table 2). The erosional surfaces bounding the seismic units (described here from older to younger units) can be followed downslope into conformable strata of the sediment waves on the upper continental slope.

The seismic unit 1 (U1) is the oldest unit identified in the seismic profiles and it is only observed on the mid-outer shelf (Fig. 5). The top of the unit is defined by the erosional surface D1 that truncates the internal reflectors of U1 (Fig. 5). Internally, the unit U1 is characterized by low-angle reflectors with onlap termination against the steeper erosional surface D1. Above, it is unit U2, which is also only observed

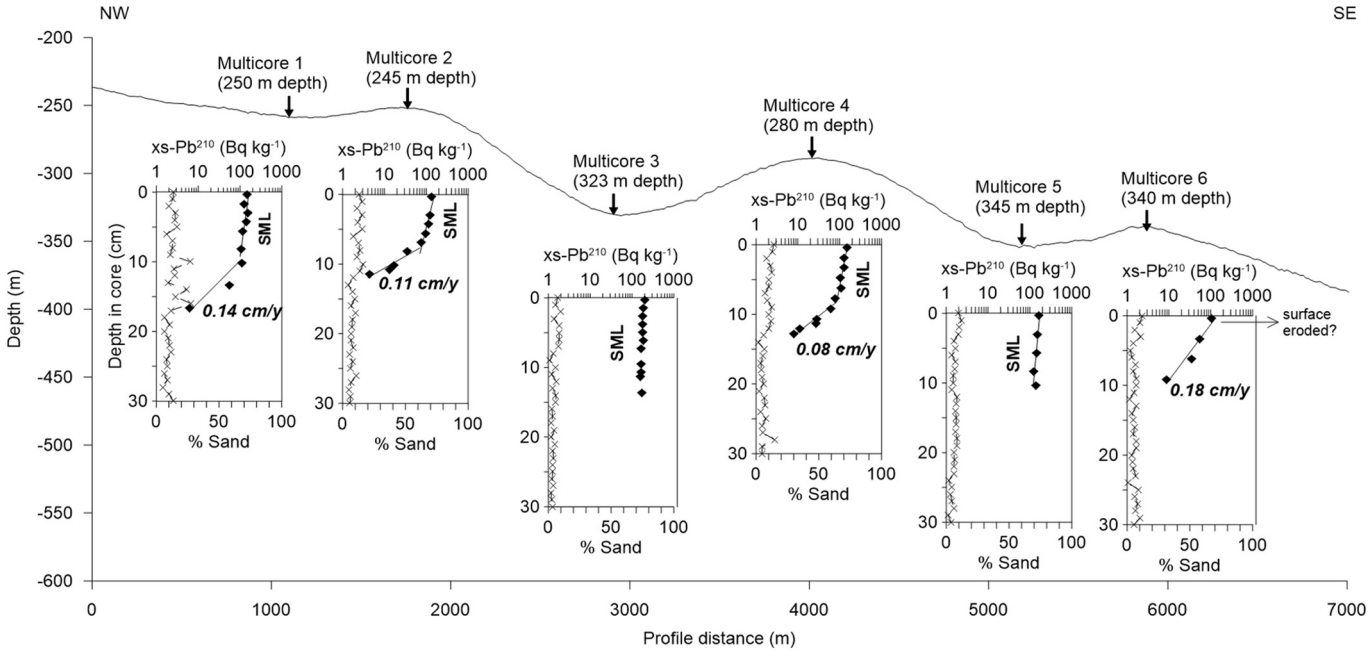

Fig. 4. Bathymetric profile following the line were the six sediment cores were collected (see location in Fig. 2). Diagrams of the grain size distribution (% sand) and the excess of ^{210}Pb (Bq/kg) are plotted for each sediment core.

Table 1
Mean characteristics of the seismic units identified over the Gulf of Roses slope, and their bounding surfaces.

Unit	Bounding surfaces		Mean min thickness (m)	Mean max thickness (m)	Presence of sediment waves
	Top	Bottom			
U7	Present-day seafloor	D6	50	100	Yes
U6	D6	D5	45	105	Yes
U5	D5	D4	30	76	Yes
U4	D4	D3	20	75	Yes
U3	D3	D2	6	25	No
U2	D2	D1	10	40	No
U1	D1	Masked by multiple	22	30	No

Table 2
Main characteristics of the sediment waves observed within the seismic units identified over the Gulf of Roses slope.

Unit	Presence of sediment waves	Mean wave height (m)	Mean wave length (m)
U7	Yes	53	2000
U6	Yes	60	2000
U5	Yes	18	1500
U4	Yes	11	1300
U3	No	–	–
U2	No	–	–
U1	No	–	–

on the mid-outer shelf, and it is limited on the top by another erosive surface, the seismic discontinuity D2. The development of sediment waves within this unit is absent, but two subunits (U2a and U2b) can be identified, showing oblique to parallel reflectors with different inclinations (Fig. 5). Over, unit U3 is identified, with the erosive surface D3 marking the top of the unit and truncating the reflectors of units U2 and U3, and also the discontinuity D2 (Fig. 5). This discontinuity D3, extends seawards and can be traced below the first multiple following a sediment wave shape, however the seismic profile resolution is not high enough to determine if sediment waves are further developed (Fig. 5).

Overhead, seismic unit U4 can be followed down to the slope, increasing in thickness downslope, from ~20 to ~75 m measurable until reaching the depth of the seismic signal penetration (Figs. 5–7; Table 1). The internal reflectors follow a steep edge, which marks the seismic unconformity D3, limiting unit U3 and U4. Sediment waves are developed downslope from the edge, with wave heights between ~5 and ~17 m and lengths of ~1300 m, decreasing in size from the base to the top of the seismic unit (Fig. 5; Table 2). Seismic discontinuity D4 separates units U4 and U5 (Fig. 5). Seismic unit U5 also shows an increase in thickness downslope, from minimum thickness of ~10 m to up to maximum of > 85 m (Fig. 5; Table 1). Sediment waves are well developed within this unit, being smaller on the outer shelf, with minimum heights of ~6 m and lengths of ~1025 m, than on the upper slope, where they present wave heights of ~30 m and lengths of ~1970 m (Fig. 5; Table 2). It should be noted that reflectors within this unit are difficult to follow since they are close to the sparker acoustic penetration limit of ~200 ms TWTT (Figs. 6–8).

Seismic discontinuity D5 marks the top of unit U5 and unit U6, which pinches out landwards on the mid-outer shelf (Fig. 5). Unit U6 increases in thickness seawards, from minimum of ~5 m on the outer shelf, to ~70 m at the upper-slope, reaching a maximum of > 120 m down the slope (Figs. 6–8; Table 1). From the shelf-edge, sediment waves start to develop, reaching heights of ~60 m and lengths of ~2000 m (Figs. 5 and 6; Table 2), tending to disappear towards the NE and downslope (Figs. 7 and 8). The top of this unit is defined by the erosive surface D6, which truncates the sediment waves on the upper slope and shelf-edge (Fig. 5).

The youngest unit U7 is topped by the present-day seafloor and shows a relatively constant thickness slightly increasing downslope from ~50 m to ~100 m (Figs. 5–8; Table 1). Sediment waves developed in this unit are very localised on the shelf-edge and upper slope, with heights of ~53 m and wave lengths of ~2000 m (Table 2), tending to disappear when the gradient of the continental slope increases (> 2°).

Over the outer continental shelf several erosional features are observed in the swath bathymetry (Fig. 2), and some are also identified in the seismic profile extending to the outer shelf (Fig. 5). This erosional feature produces local erosional truncation of the subsurface reflectors of unit U7 (Fig. 5). Additionally, the presence of pockmarks identified

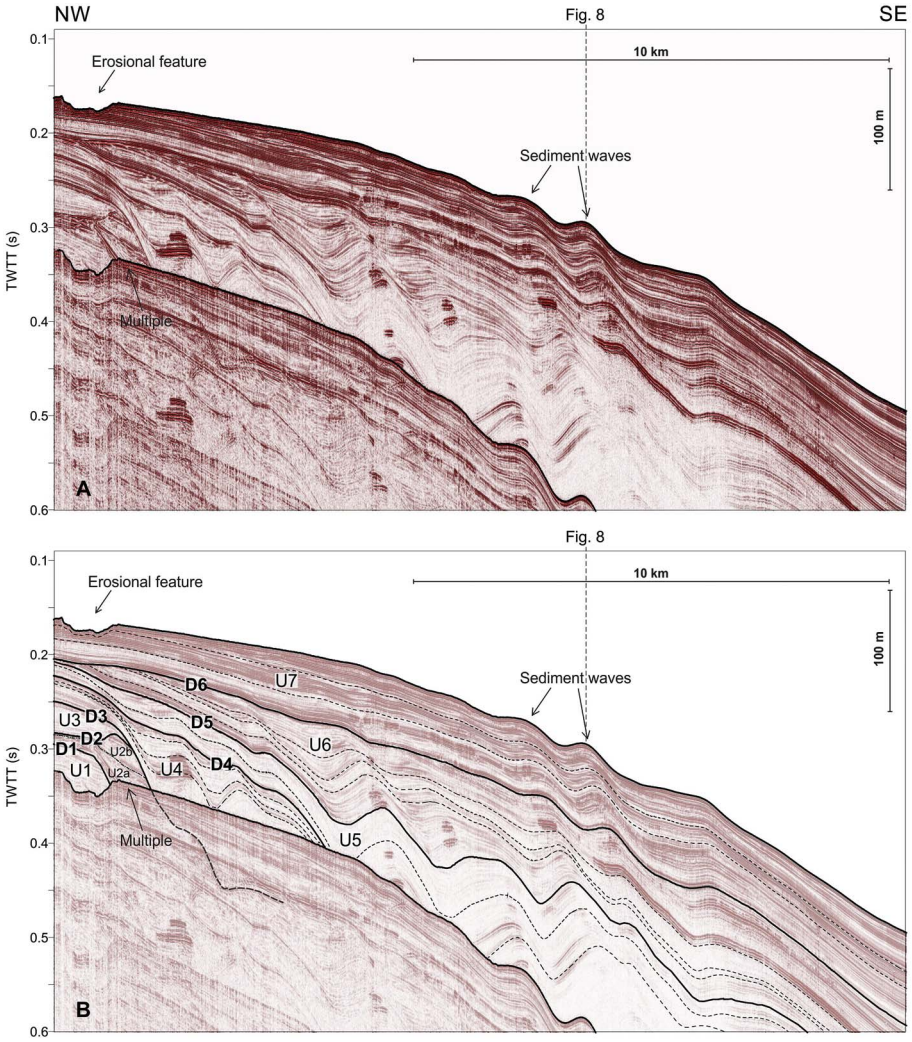

Fig. 5. **A**) Single-channel (sparker) reflection seismic profile crossing perpendicular to the sediment waves (see location in Fig. 2). **B**) Interpretation of the seismic profile. Unconformities D1 to D6 limiting the seismic units from U1 to U7 are marked with solid lines, and dashed lines follow selected horizons within each unit. Modified from Ribó et al. (2017).

on the bathymetric data (Fig. 3A), is also evidenced on the seismic profiles, and associated with a thin column of acoustic blanking throughout the seismic profile (Fig. 8). Moreover, the seismic profiles along the sediment waves (Fig. 8) reaching the Cap de Creus submarine canyon SW flank (see location in Fig. 2), show a sediment accumulation at the rim of canyon (i.e., a levee-like deposit), that can locally reach heights of ~14 m over the present sea floor (Fig. 8).

4. Discussion

4.1. Sediment wave development over the Gulf of Roses continental slope

Erosive and depositional features over the southwestern GoL and GoR continental shelf and slope have been related to the DSW flows across- and along-margin (Lastras et al., 2011; Lo Iacono et al., 2012; Durán et al., 2014). Several studies have demonstrated that the combination of storm-induced downwelling and DSWC events increase the bottom currents and induce active sediment resuspension and transport from the shelf to the slope, predominantly through the Cap de Creus submarine canyons (Palanques et al., 2006, 2008, 2012; Puig et al., 2008; Ulses et al., 2008a, 2008b, 2008c; Ribó et al., 2011; Martín et al., 2013). During such events, suspended sediment is also advected southwards along the shelf, off the Cap de Creus promontory, towards the GoR (Bourrin et al., 2008; Ogston et al., 2008; Ulses et al., 2008b; DeGeest et al., 2008; Ribó et al., 2011). In this area, the formation of the erosive and depositional features over the shelf and slope depends on the orientation of the flow relative to the regional bathymetry, the presence of the Cap de Creus promontory, the submarine canyon heads incising the margin, and the pre-existing features, such as rocky ridges and shoals (Lastras et al., 2007; Lo Iacono et al., 2012; Durán et al., 2014). The presence of erosive features, such as the Roses Channel (Fig. 2), evidences the overflow of dense waters towards the GoR shelf. This channel has been interpreted as a mixed erosional-depositional feature, that occasionally provides an escape route for northern waters that are not trapped by the canyon head, flowing southwards surrounding the Cap de Creus promontory (Durán et al., 2014). However, the sediment waves recently identified over the upper slope suggest that a major part of the sediment transported within the DSW can also be transferred across the continental slope.

In the GoR, the currents enhanced during DSWC events are mainly along-shelf currents, but have also an across-shelf component, enhancing the downslope sediment transport (Ulses et al., 2008a). This is possible since friction created on the seabed by the along-shelf currents can break the constraint of potential vorticity conservation (which requires all motion to be along-shelf/slope), permitting cross-isobath motions, and thus, generate downslope currents (Shapiro and Hill, 1997). The existing numerical simulations (Ulses et al., 2008a) and hull-mounted Acoustic Doppler Current Profiler observations (DeGeest et al., 2008, their Fig. 4), combined with the new bathymetric data here presented, reveal that the location where the sediment wave field

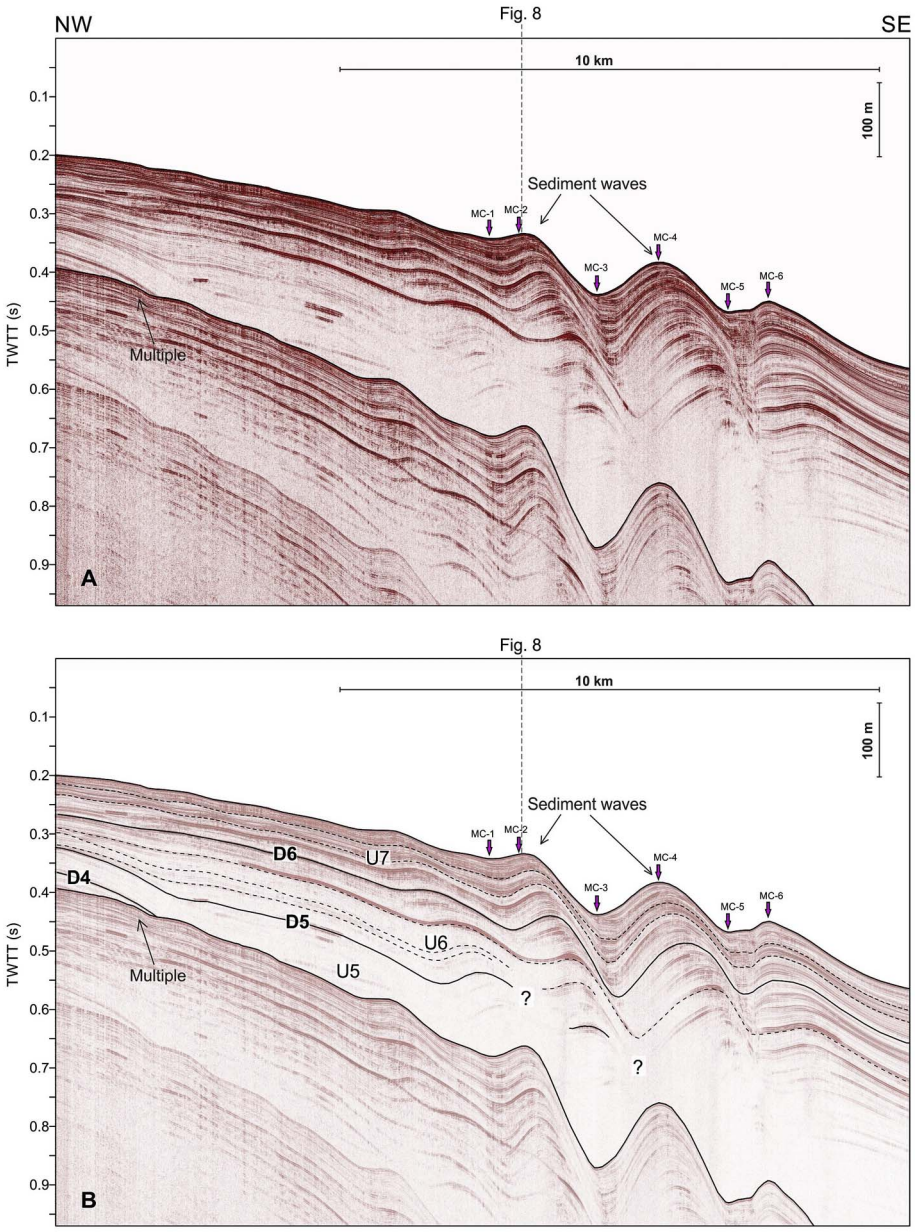

Fig. 6. **A**) Single-channel (sparker) reflection seismic profile crossing perpendicular to the sediment waves and indicating the location of the collected sediment samples (MC-1 to MC-6) (see location in Fig. 2). **B**) Interpretation of the seismic profile. Unconformities D3, D4 and D5 limiting the seismic units from U3 to U6 are marked with solid lines, and dashed lines follow selected horizons within each unit. Question marks indicate areas where internal reflectors could not be followed.

develops is aligned with the path of the dense water plume bypassing the Cap de Creus promontory and cascading over the GoR slope (Fig. 2). Moreover, the orientation of the sediment waves on the upper slope is almost parallel to the regional slope, and perpendicular to the bottom current flow. This evidences that the bottom currents enhanced by the DSW flowing cross-slope are most likely to be the formation process developing the sediment waves over the GoR continental slope. Downslope, the sediment waves orientation changes from NNE-SSW to NE-SE, becoming oblique to the regional bathymetry (Fig. 3A). It is here hypothesized that the change on the sediment wave orientation is forced by the effect of the dense waters cascading downslope coming across with the Northern Current, flowing southwards along the upper slope (Fig. 1). This would force the DSWC and the enhanced bottom currents forming the sediment waves to change the orientation (Figs. 2 and 3A).

Furthermore, the sediment waves observed over the GoR slope share common characteristics with the ones described worldwide to be formed by bottom currents enhanced by DSWC: a) isolated and very localised fields; b) upslope asymmetry; c) irregular distribution of wave sizes; d) occurrence and development of the sediment wave fields near sharp edges (Verdicchio and Trincardi, 2006; Anderskouv et al., 2010; Foglini et al., 2016). The limited depth range where the sediment waves are developed, between ~200 and ~400 m water depth (Fig. 2), indicates the equilibrium density depth reached by the downslope currents over the GoR slope. The short lateral continuity of the wave crests (Fig. 3A) and the specific location of the sediment wave field over the upper continental slope (Fig. 2), suggest that the sediment waves are affected by a bottom-trapped flow of dense waters cascading off the shelf. The sediment waves over the GoR slope characterized in this study, contributes to better understand the DSWC processes and associated off-shelf sediment transport reshaping the morphology of open-slopes.

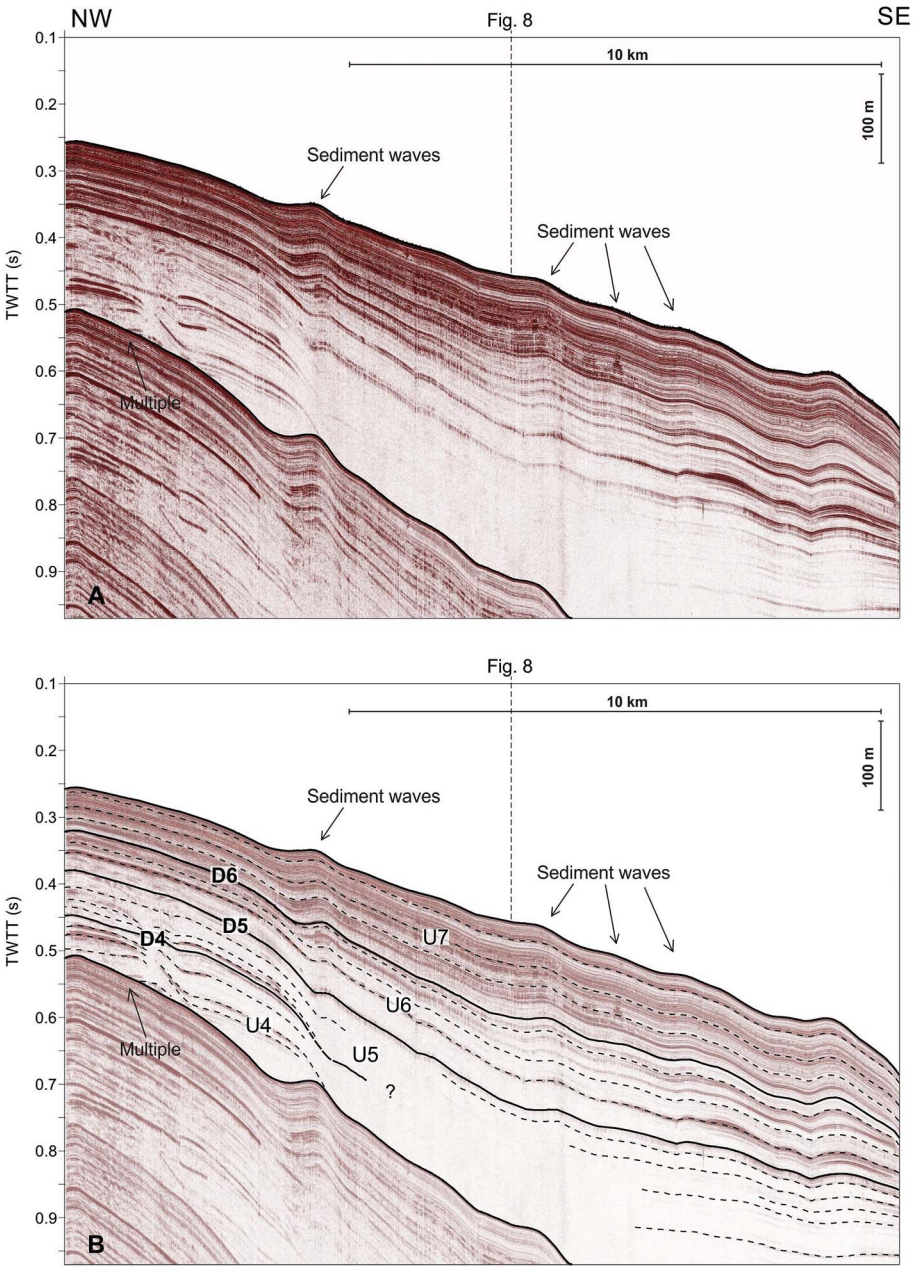

Fig. 7. A) Single-channel (sparker) reflection seismic profile crossing perpendicular to the sediment waves and the contourite deposit (see location in Fig. 2). **B**) Interpretation of the seismic profile. Unconformities D4, D5 and D6 limiting the seismic units from U4 to U7 are marked with solid lines, and dashed lines follow selected horizons within each unit. Question marks indicate areas where internal reflectors could not be followed.

4.2. Chrono-stratigraphy of the Gulf of Roses continental shelf and slope

In the Northern Catalan margin, the Late Pleistocene-Holocene sedimentary evolution has been mainly controlled by both transgressive and highstand stages of the last eustatic sea-level cycle (Tassone et al., 1996; Ercilla, 1992; Ercilla et al., 1994, 1995; García et al., 2011). During the last decade, many interpretations of erosive surfaces correlated to the Pleistocene sea-level variations have been discussed in the nearby GoL, north of GoR, and are summarized by Rabineau et al. (2005).

The stratigraphic sequence of the Late Pleistocene of the GoL (Fig. 1), has been intensively studied through seismic investigations and dated sediment cores (Rabineau et al., 2005, 2006; Bassetti et al., 2008; Sierro et al., 2009). Major seismic discontinuities have been identified as sequence boundaries at the top of prograding wedges throughout the GoL shelf, corresponding to 100-ka glacioeustatic cycles (i.e., discontinuities D40, D50 and D60 correspond to the Marine Isotope Stages, MIS-10 (~340 ka), MIS-8 (~240 ka) and MIS-6 (~130 ka)) (Rabineau et al., 2005, 2006; Bassetti et al., 2008).

In the Barcelona continental shelf, south of the GoR (Fig. 1), Liquete et al. (2008) described five unconformity-bounded seismic units, correlating the deepest sequence boundary to MIS-10 (~340 ka) and the shallowest one to MIS-2 (~14 ka).

In the GoR continental shelf, the development of the Pleistocene deposits was first described by Ercilla et al. (1994) and interpreted to be mainly controlled by high-frequency sea level changes. In the results here presented, seven seismic units (U1–U7) are differentiated through the sedimentary record (Figs. 5–8), separated by erosional surfaces (D1–D6), presumably formed by the subaerial erosion during the sea level falls. The erosional surface D2 (Fig. 5) can be correlated to the reflector J identified by Ercilla et al. (1994) on the outer continental shelf (their Fig. 5A). However, it seems very unlikely that this reflector

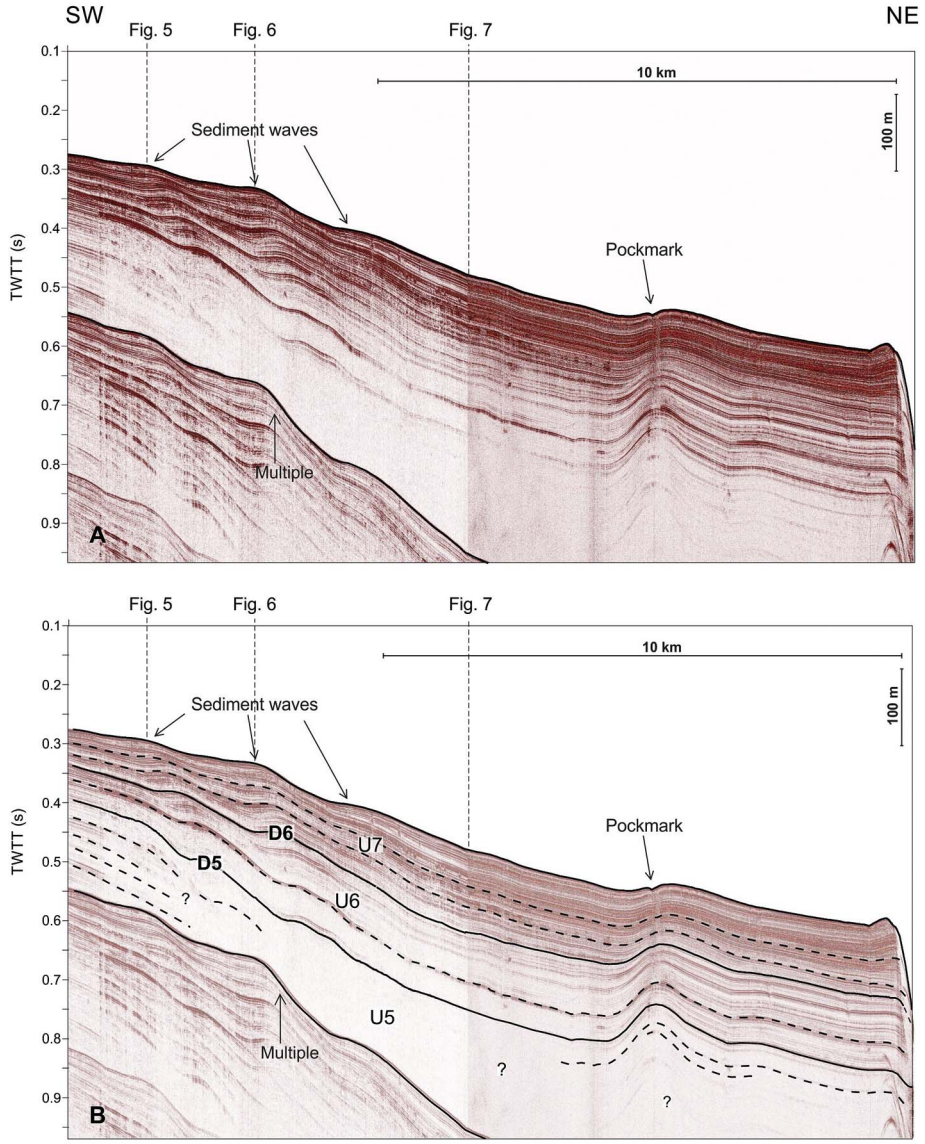

Fig. 8. **A**) Single-channel (sparker) reflection seismic profile along the sediment waves and crossing a pockmark and reaching the edge of the Cap de Creus submarine canyon southern flank (see location in Fig. 2). **B**) Interpretation of the seismic profile. Unconformities D5 and D6 delimiting the seismic units from U4 to U7 are marked with solid lines, and dashed lines follow selected horizons within each unit. Question marks indicate areas where internal reflectors could not be followed.

had been developed during Termination II (transition between MIS-6 and MIS-5.5, ~120 ka), when comparing the seismic stratigraphy of the GoR with the GoL (Rabineau et al., 2005, 2006; Bassetti et al., 2008). The upper Quaternary stratigraphic sequence thickness described in the GoL shelf edges is approx. ~150 ms TWTT thick (Rabineau et al., 2005, 2006). The GoR stratigraphic sequence thickness is determined in this study, being also ~150 ms TWTT thick (Fig. 5). However, the lack of major rivers discharging large amounts of sediment over the shelf (Durán et al., 2014) suggests that the accumulation rates in the GoR continental shelf should be lower than in the GoL shelf. Thus, it seems doubtful that the erosive surface over the GoR shelf, identified as reflector J by Ercilla et al. (1994), placed at ~200 m water depth, could been developed at ~120 ka.

Therefore, although absolute dates are not available for the GoR margin, a new chronostratigraphic interpretation for the erosive surfaces limiting the seismic units over the GoR shelf is here proposed. It is assumed that the architecture and the unconformity-bounded depositional sequences forming the GoR shelf and slope are comparable to the stratigraphy described on the GoL shelf. The seismic line shown in Fig. 5 is used for the sequence stratigraphic interpretation because it extends to the mid and inner shelf (see Fig. 2). The identified units U1, U2 and U3 show relative flat reflectors with no clear sediment wave development, in contrast with all the above units (U4 to U7), indicating a possible change in the hydrodynamic conditions. The reflectors of U2 and U3 are sharply truncated, as well as the discontinuity D2, by the seismic discontinuity D3 (Fig. 5). This steep and sharp erosive surface (D3) is here related to the erosion process during MIS-10 lowstand, according to the pronounced sea level drop, reaching a minimum of ~150 m below the present sea level in the nearby GoL (Rabineau et al., 2006). This unconformity is placed at ~180 m water depth, which is consistent with the observations in the north, on GoL shelf, where it is identified at ~250 m (Rabineau et al., 2005).

Following the criteria that the defined unit boundaries can be interpreted as erosional surfaces created during 4th order sea-level falls (~100 ka), MIS-8 (~240 ka) and MIS-6 (~130 ka) probably correspond to the erosive surfaces D4, and D6, respectively (Fig. 5). Although there is a lack of age control, the proposed chronostratigraphic interpretation correlates well with the observations from the GoL continental shelf (Rabineau et al., 2005).

4.3. Sedimentary processes during the GoR continental margin evolution

The sediment waves over the GoR continental slope were initially interpreted as slump and creep features by Ercilla et al. (1994). These authors described the development of instability features in the outer continental shelf and shelf-break to be favoured by the relatively steep seabed gradients and high sediment supply, uplifting of the Cap de Creus peninsula (Medialdea et al., 1994). However, the seismic data presented in this paper shows continuous internal reflectors which can be traced across the crests and troughs of each sediment wave along the high-resolution single-channel seismic profiles, with no shear planes being identified (Figs. 5–7). Moreover, the bathymetric data shows total absence of headwall scarp from where a possible slump would have been initiated, and no compressional features at the toe of the sediment wave field are observed, which would be expected at the base of an instability feature (Fig. 2). Additionally, from the chrono-stratigraphic approach, it is assumed that the sediment wave field has been constructed over a long-time period and involve sediment deposition from several events (Figs. 5–7). It should also be noted that all seismic units are continuous beyond the sediment-wave field into areas of parallel reflectors, with no discontinuities (e.g., faults) surrounding the sediment wave field (e.g., upstream or downstream) (Figs. 2 and 5–7). These observations allowed excluding the possibility that deformation was occurring at the time the sediment was deposited in the area (Lee et al., 2002). From the bathymetric data it can be observed that the sediment waves are irregular, and the sediment wave crests orientation is oblique to the regional slope, which follow the criteria to identify bottom current sediment waves (Wynn and Stow, 2002).

As stated above, the development sediment waves over the upper GoR slope is here interpreted to be formed by bottom currents enhanced by DSW cascading down the slope. The different sediment wave heights and lengths observed within the different seismic units (Figs. 5–7), suggests successive DSWC events supplied uneven volume of sediment downslope, irregularly through time, depending on the intensity of the cascading flows. Similarly, the thick sedimentary body (PLSR; Fig. 1) identified down the slope is characterized by the presence of sediment waves identified within several sets (units), showing cyclic variations of sedimentation (Jallet and Giresse, 2005). The authors suggested that DSWC events could be responsible for part of the overflows from the Cap de Creus canyon, representing a nearly continuous background of sediment deposition. As with the sediment waves observed over the GoR, the thick deposits identified within the PLSR on the lower slope were suggested to correspond to periods of important terrigenous supplies, linked to major low-stand intervals (Jallet and Giresse, 2005).

The sediment cores collected on the sediment waves over the GoR slope show that the cores collected over the sediment wave crests (MC-2 and 4) have higher sand fraction on the upper 10 cm than the cores collected the troughs (MC-3 and 5), suggesting a different sediment accumulation pattern (Fig. 4). However, most of the cores present a thick surface mixed layer and an increase of the sand fraction in the upper sections, suggesting that the surface sediments over the slope are affected by bottom trawling activities (Fig. 3B). Trawling gear will stir and mix the surface sediment and cause resuspension and winnowing of finer particles that are transported away, while coarser particles remain. The deeper core collected at 340 m water depth (MC-6, see location in Fig. 2) does not show a mixed layer (Fig. 4), but surface ^{210}Pb activities suggest that this core could have been eroded. Overall, the sedimentation rates that could be derived from the collected sediment cores do not show differential sediment deposition rates between sediment wave crests and troughs, leaving unclear if the sediment waves are still active and growing, but the recent sedimentation is altered by bottom trawling, or if they are currently inactive and covered by a thin veneer of draping sediments. Longer sediment cores will be necessary to clarify this aspect.

Nevertheless, the data obtained from the collected sediment samples, combined with the swath bathymetry and the seismic profiles, indicate that the slope bottom currents enhanced during DSWC events have apparently been continuously shaping the GoR slope through the Pleistocene, with presumably continuous sediment deposition affected by the eustatic oscillations. Although there is a high anthropogenic disturbance over the continental shelf and upper slope, natural processes such as bottom currents are the most likely main mechanism for the sediment wave development.

5. Conclusions

New acquired swath bathymetry and seismic profiles revealed the presence of large sediment waves over the GoR continental slope, extending from ~200 m to ~400 m water depth, previously related to slump or creep-like deformation. It is here suggested that the bottom currents advecting suspended sediments down the open slope during major DSWC events are the most probable formation mechanisms for the observed sediment waves.

A new chronostratigraphic interpretation over the GoR shelf is here proposed. Seven seismic units are differentiated throughout the sedimentary record, separated by major seismic discontinuities that are interpreted as erosional surfaces created during 4th order sea-level falls (MIS-10 (340 ka), MIS-8 (~240 ka) and MIS-6 (~130 ka)). Despite the lack of age control, the proposed chronostratigraphic interpretation correlates well with the stratigraphy described on the GoL continental shelf.

The sediment waves are developed within the Quaternary, particularly within the youngest seismic units (U4-U7), indicating that DSWC events have been occurring in this margin since about 340 ka (shortly after MIS-10). The differences in height and length of the sediment waves within the different seismic units, suggest variations in the sediment transferred through time, as well as in the bottom current magnitude and direction enhanced during DSWC events.

Data analysed in this work indicate that despite there is high anthropogenic impact over the GoR continental shelf and upper slope at present-day, the continuous formation of sediment waves throughout the sedimentary record suggest continuous sediment deposition most probably driven by natural process, such as bottom currents enhanced by the DSWC events over long-time scales.

The morphological and stratigraphic analysis presented in this paper provides new insights to better understand the impact of the DSWC on shaping the seafloor over continental slopes worldwide.

Acknowledgments

This work was funded by the Spanish grants FORMED (CGL2012-33989) and ABIDES (CTM2015-65142-R) and by the Generalitat de Catalunya supporting grants 2014 SGR-1642 and 2014 SGR-1356. The authors wish to thank the captain and the crew of the R/V García del Cid, and also the UTM technicians and the Instrumental Service, J. Pozo and M. Lloret, for their assistance. The authors are very grateful for the effort made by the two reviewers to improve the quality of thispaper, and especially wish to thank the comments made by Serge Berné.

References

Anderskouv, K., Surlyk, F., Huuse, M., Lykke-Andersen, H., Bjerager, M., Tang, C.D., 2010. Sediment waves with a biogenic twist in Pleistocene cool water carbonates, Great Australian Bight. Mar. Geol. 278, 122–139.

Bassetti, M.A., Berné, S., Jouet, G., Taviani, M., Dennielou, B., Flores, J.-A., Gaillot, A., Gelfort, R., Lafuerza, S., Sultan, N., 2008. The 100-ka and rapid sea level changes recorded by prograding shelf sand bodies in the Gulf of Lions (western Mediterranean Sea). Geochem. Geophys. Geosyst. G^3 9 (11). http://dx.doi.org/10.1029/2007GC001854.

Berné, S., Loubrieu, B., 1999. Canyons and recent sedimentary processes on the western Gulf of Lions margin. First results of the Calmar cruise. C. R. Acad. Sci. 328 (7), 471–477.

Béthoux, J., Durrieu de Madron, X., Nyffeler, F., Tailliez, D., 2002. Deep water in the

western Mediterranean: peculiar 1999 and 2000 characteristics, shelf formation hypothesis, variability since 1970 and geochemical inferences. J. Mar. Syst. 33–34, 117–131.
Bourrin, F., Friend, P.L., Amos, C.L., Manca, E., Ulses, C., Palanques, A., Durrieu de Madron, X., Thompson, C.E.L., 2008. Sediment dispersal from a typical Mediterranean flood: the Têt River, Gulf of Lions. Cont. Shelf Res. 28, 1895–1910.
Canals, M., Puig, P., Durrieu de Madron, X., Heussner, S., Palanques, A., Fabres, J., 2006. Flushing submarine canyons. Nature 444, 354–357.
Canals, M., Danovaro, R., Heussner, S., Lykousis, V., Puig, P., Trincardi, F., Calafat, A.M., Durrieu de Madron, X., Palanques, A., Sanchez-Vidal, A., 2009. Cascades in Mediterranean submarine grand canyons. Oceanography 22 (1), 26–43.
Canals-Artigas, M., 1985. Estructura sedimentaria y evolución morfológica del talud y el glacis continental del Golfo de Leon: fenómenos de desestabilización de la cobertera sedimentaria plio-cuaternaria (PhD Thesis). Universitat de Barcelona, pp. 618.
Cattaneo, A., Correggiari, A., Marsset, T., Thomas, Y., Marsset, B., Trincardi, F., 2004. Seafloor undulation pattern on the Adriatic shelf and comparison to deep-water sediment waves. Mar. Geol. 213, 121–148.
DeGeest, A.L., Mullenbach, B.L., Puig, P., Nittrouer, C.A., Drexler, T.M., Durrieu de Madron, X., Orange, D.L., 2008. Sediment accumulation in the western Gulf of Lions, France: the role of Cap de Creus Canyon in linking shelf and slope sediment dispersal systems. Cont. Shelf Res. 28, 2031–2047.
Delivet, S., Van Eetvelt, B., Monteys, X., Ribó, M., Van Rooij, D., 2016. Seismic geomorphological reconstructions of Plio-Pleistocene bottom current variability at Goban Spur. Mar. Geol. 378, 261–275.
Durán, R., Canals, M., Sanz, J.L., Lastras, G., Amblàs, D., Micallef, A., 2014. Morphology and sediment dynamics of the northern Catalan continental shelf, northwestern Mediterranean Sea. Geomorphology 204, 1–20.
Durrieu de Madron, X., Nyffeler, F., Gode, C.H., 1990. Hydrographic structure and nepheloid spatial distribution in the Gulf of Lions. Cont. Shelf Res. 28, 1920–1934.
Durrieu de Madron, X., Zervakis, V., Theocharis, A., Georgopoulos, D., 2005. Comments on “Cascades of dense water around the world ocean”. Prog. Oceanogr. 64, 83–90.
Durrieu de Madron, X., Wiberg, P.L., Puig, P., 2008. Sediment dynamics in the Gulf of Lions: the impact of extreme events. Cont. Shelf Res. 28, 1867–1876.
Ercilla, G., 1992. La sedimentación Cuaternaria en márgenes y cuencas del Mediterráneo noroccidental y suroccidental: Modelos de evolución sedimentaria y factores de control (PhD Thesis). Universitat de Barcelona, pp. 567.
Ercilla, G., Farrán, M., Alonso, B., Díaz, J.I., 1994. Pleistocene progradational growth pattern of the northern Catalonia continental shelf (northwestern Mediterranean). Geo-Mar. Lett. 14 (4), 264–271.
Ercilla, G., Díaz, J.I., Alonso, B., Farrán, M., 1995. Late Pleistocene-Holocene sedimentary evolution of the northern Catalonia continental shelf (northwestern Mediterranean Sea). Cont. Shelf Res. 15, 1435–1451.
Farrán, M., 2005. Catalano-Balearic Sea (NW Mediterranean) – Bathymetric Chart and Toponyms. Available at. http://gma.icm.csic.es/sites/default/files/geowebs/MCB/CBSmaps.htm (Accessed 1st of February 2016).
Faugères, J.–C., Gonthier, E., Mulder, T., Kenyon, N., Cirac, P., Griboulard, R., Berné, S., Lesuavé, R., 2002. Multi-process generated sediment waves on the Landes Plateau (Bay of Biscay, North Atlantic). Mar. Geol. 182, 279–302.
Fieux, M., 1974. Formation d'eau dense sur le plateau du golfe du Lion. In: Processus de formation des eaux profondes. Colloques Internationaux du, CNRS 215, pp. 165–174.
Flexas, M.M., Durrieu de Madron, X., García, M.A., Canals, M., Arnau, P., 2002. Flow variability in the Gulf of Lion during the MATER HFF experiment (March–May 1997). J. Mar. Syst. 33-34, 197–214.
Foglini, F., Campiani, E., Trincardi, F., 2016. The reshaping of the South West Adriatic Margin by cascading of dense shelf waters. Mar. Geol. 375, 64–81.
Fohrmann, H., Backhaus, J.O., Blaume, F., Rumohr, J., 1998. Sediments in bottom-arrested gravity plumes: numerical case studies. J. Phys. Oceanogr. 28, 2250–2274.
Font, J., Garcia-Ladona, E., Gorriz, E.G., 1995. The seasonality of mesoscale motion in the northern current of the western Mediterranean several years of evidence. Oceanol. Acta 18, 207–219.
García, M., Maillard, A., Aslanian, D., Rabineau, M., Alonso, B., Gorini, C., Estrada, F., 2011. The Catalan margin during the Messinian salinity crisis: physiography, morphology and sedimentary record. Mar. Geol. 284, 158–174.
Got, H., 1973. Etude des correlations tectonique-sedimentation au cours de l'historie Quaternaire du Precontinent Pyreneo-Catalan (PhD Thesis). Université des Sciences et Techniques du Languedoc, pp. 294.
IOC, IHO, BODC, 2003. Centenary Edition of the GEBCO Digital Atlas, Published on CDROM on Behalf of the Intergovernmental Oceanographic Commission and the International Hydrographic Organization as Part of the General Bathymetric Chart of the Oceans. Dat. British Oceanographic.
Ivanov, V.V., Shapiro, G.I., Huthnance, J.M., Golovin, D.L., Aleynik, P.N., 2004. Cascades of dense water around the world ocean. Prog. Oceanogr. 60, 47–98.
Jallet, L., Giresse, P., 2005. Construction of the Pyreneo-Languedocian sedimentary ridge and associated sediment waves in the deep western Gulf of Lions (Western Mediterranean). Mar. Pet. Geol. 22, 865–888.
Krishnaswamy, S., Lal, D., Martin, J., Meybeck, M., 1971. Geochronology of lake sediments. Earth Planet. Sci. Lett. 11, 407–414.
La Violette, P.E., Tintoré, J., Font, J., 1990. The surface circulation of the Balearic Sea. J. Geophys. Res. 98, 1377–1398.
Lastras, G., Canals, M., Urgeles, R., Amblas, D., Ivanov, M., Droz, L., Dennielou, B., Fabrés, J., Schoolmeester, T., Akhmetzhanov, A., Orange, D., García-García, A., 2007. A walk down the Cap de Creus canyon, Northwestern Mediterranean Sea: recent processes inferred from morphology and sediment bedforms. Mar. Geol. 246, 176–192.
Lastras, G., Canals, M., Amblas, D., Lavoie, C., Church, I., De Mol, B., Duran, R., Calafat, A.M., Hughes-Clarke, J.E., Smith, C.J., Heussner, S., “Euroleón” cruise shipboard party, 2011. Understanding sediment dynamics of two large submarine valleys from seafloor data: Blanes and La Fonera canyons, northwestern Mediterranean Sea. Mar. Geol. 280, 20–39.
Lee, H.J., Syvitski, J.P.M., Parker, G., Orange, D., Locat, J., Hutton, J.H.W., Imran, J., 2002. Distinguishing sediment waves from slope failure deposits: field examples, including the “Humboldt Slide” and modelling results. Mar. Geol. 192, 79–104.
Liquete, C., Canals, M., De Mol, B., De Batist, M., Trincardi, F., 2008. Quaternary stratal architecture of the Barcelona prodeltaic continental shelf (NW Mediterranean). Mar. Geol. 250, 234–250.
Lo Iacono, C., Guillén, J., Puig, P., Ribó, M., Ballesteros, M., Palanques, A., Farrán, M., Acosta, J., 2010. Large-scale bedforms along a tideless outer shelf setting in the western Mediterranean. Cont. Shelf Res. 30, 1802–1813.
Lo Iacono, C., Orejas, C., Gori, A., Gili, J.M., Requena, S., Puig, P., Ribó, M., 2012. Habitats of the Cap de Creus continental shelf and Cap de Creus Canyon, Northwestern Mediterranean. In: Harris, P.T., Baker, E.K. (Eds.), Seafloor Geomorphology as Benthic Habitat: GeoHAB Atlas of Seafloor Geomorphic Features and Benthic Habitats. Elsevier, Amsterdam, pp. 457–469.
Maillard, A., Mauffret, A., Watts, A.B., Torné, M., Pascal, G., Buhl, P., Pinet, B., 1992. Tertiary sedimentary history and structure of the Valencia Trough (Western Mediterranean). Tectonophysics 203, 57–76.
Martín, J., Palanques, A., Puig, P., 2006. Composition and variability of downward particulate matter fluxes in the Palamós submarine canyon (NW Mediterranean). J. Mar. Syst. 60, 75–97.
Martín, J., Palanques, A., Puig, P., 2007. Horizontal transfer of suspended particulate matter in the Palamós submarine canyon. J. Mar. Res. 65, 193–218.
Martín, J., Puig, P., Palanques, A., Masqué, P., García-Orellana, J., 2008. Effect of commercial trawling on the deep sedimentation in a Mediterranean submarine canyon. Mar. Geol. 252, 150–155.
Martín, J., Durrieu de Madron, X., Puig, P., Bourrin, F., Palanques, A., Houpert, L., Higueras, M., Sanchez-Vidal, A., Calafat, A.M., Canals, M., Heussner, S., 2013. Sediment transport along the Cap de Creus Canyon flank during a mild, wet winter. Biogeosciences 10, 3221–3239.
Martín, J., Puig, P., Palanques, A., Ribó, M., 2014. Trawling-induced daily sediment resuspension in the flank of a Mediterranean submarine canyon. Deep-Sea Res. II 104, 174–183.
Masqué, P., Isla, E., Sanchez-Cabeza, J.A., Palanques, A., Bruach, J.M., Puig, P., Guillén, J., 2002. Sediment accumulation rates and carbon fluxes to bottom sediments at the Western Bransfield Strait (Antarctica). Deep-Sea Res. II Top. Stud. Oceanogr. 49, 921–933.
Masson, D.G., Howe, J.A., Stoker, M.S., 2002. Bottom-current sediment waves, sediment drifts and contourites in the northern Rockall Trough. Mar. Geol. 192, 215–237.
Medialdea, J., Maldonado, A., Alonso, B., Díaz, J.I., Ercilla, G., Farrán, M., Medialdea, T., Vázquez, T., 1994. Mapa geológico de la plataforma continental española y zonas adyacentes. 1:200.000. Memoria y Hojas num. 25 y 25E. Figueres, Servicio de Publicaciones del Ministerio de Industria y Energía, Madrid.
Mendoza, E.T., Jimenez, J.A., Mateo, J., 2011. A coastal storm intensity scale for the Catalan Sea (NW Mediterranean). Nat. Hazards Earth Syst. Sci. 11, 2453–2462. http://dx.doi.org/10.5194/nhess-11-2453-2011.
Millot, C., 1999. Circulation in the Western Mediterranean Sea. J. Mar. Syst. 20, 423–442.
Mosher, D.C., Thomson, R.E., 2002. The foreslope hills: large-scale, fine-grained sediment waves in the Strait of Georgia, British Columbia. Mar. Geol. 192, 275–295.
Muñoz, J.A., Martínez, A., Vergés, J., 1986. Thrust sequences in the eastern Spanish Pyrenees. J. Struct. Geol. 8, 399–405.
Nittrouer, C.A., DeMaster, D.J., McKee, B.A., Cutshall, N.H., Larsen, I.L., 1984. The effect of sediment mixing on Pb-210 accumulation rates for the Washington continental shelf. Mar. Geol. 54, 201–221.
Ogston, A.S., Drexler, T.M., Puig, P., 2008. Sediment delivery, resuspension, and transport in two contrasting canyon environments in the southwest Gulf of Lions. Cont. Shelf Res. 28, 2000–2016.
Palanques, A., Durrieu de Madron, X., Puig, P., Fabres, J., Guillén, J., Calafat, A., Canals, M., Heussner, S., Bonnin, J., 2006. Suspended sediment fluxes and transport processes in the Gulf of Lions submarine canyons. The role of storms and dense water cascading. Mar. Geol. 234, 43–61.
Palanques, A., Guillén, J., Puig, P., Durrieu de Madron, X., 2008. Storm-driven shelf-to-canyon suspended sediment transport at the southwestern Gulf of Lions. Cont. Shelf Res. 28, 1947–1956.
Palanques, A., Puig, P., Guillén, J., Durrieu de Madron, X., Latasa, M., Scharek, R., Martín, J., 2011. Effects of storm events on the shelf-to-basin sediment transport in the southwestern end of the Gulf of lions (northwestern Mediterranean). Nat. Hazards Earth Syst. Sci. 11, 843–850.
Palanques, A., Puig, P., Durrieu de Madron, X., Sanchez-Vidal, A., Pasqual, C., Martín, J., Calafat, A., Heussner, S., Canals, M., 2012. Sediment transport to the deep canyons and open-slope of the western Gulf of Lions during the 2006 intense cascading and open-sea convection period. Prog. Oceanogr. 106, 1–15.
Paradis, S., Puig, P., Masqué, P., Juan-Díaz, X., Martín, J., Palanques, A., 2017. Bottom-trawling along submarine canyons impacts deep sedimentary regimes. Sci. Rep. 7, 43332.
Puig, P., Palanques, A., Orange, D.L., Lastras, G., Canals, M., 2008. Dense shelf water cascades and sedimentary furrow formation in the Cap de Creus Canyon, northwestern Mediterranean Sea. Cont. Shelf Res. 28, 2017–2030.
Puig, P., Canals, M., Company, J.B., Martín, J., Amblas, D., Lastras, G., Palanques, A., 2012. Ploughing the deep-sea floor. Nature 489, 286–289.
Puig, P., Durrieu de Madron, X., Salat, J., Schroeder, K., Martín, J., Karageorgis, A.P., Palanques, A., Roullier, F., Lopez-Jurado, J.L., Emelianov, M., Moutin, T., Houpert, L., 2013. Thick bottom nepheloid layers in the western Mediterranean generated by deep dense shelf water cascading. Prog. Oceanogr. 111, 1–23.

Puig, P., Martín, J., Masqué, P., Palanques, A., 2015. Increasing sediment accumulation rates in La Fonera (Palamós) submarine canyon axis and their relationship with bottom-trawling activities. Geophys. Res. Lett. 42, 8106–8113.
Rabineau, M., Berné, S., Aslanian, D., Olivet, J.-L., Joseph, P., Guillocheau, F., Bourillet, J.-F., Ledrezen, E., Granjeon, D., 2005. Sedimentary sequences in the Gulf of Lion: a record of 100,000 years of climatic cycles. Mar. Pet. Geol. 22 (6–7), 775–804.
Rabineau, M., Berné, S., Olivet, J.-L., Aslanian, D., Guillocheau, F., Joseph, P., 2006. Paleo sea levels reconsidered from direct observation of paleoshoreline position during glacial maxima (for the last 500,000 yr). Earth Planet. Sci. Lett. 252, 119–137.
Reeder, B.D., Ma, B.B., Yang, J.Y., 2011. Very large subaqueous sand dunes on the upper continental slope in the South China Sea generated by episodic, shoaling deep-water internal solitary waves. Mar. Geol. 279, 12–18.
Ribó, M., Puig, P., Palanques, A., Lo Iacono, C., 2011. Dense shelf water cascades in the Cap de Creus and Palamós submarine canyons during winters 2007 and 2008. Mar. Geol. 284, 175–188.
Ribó, M., Puig, P., Muñoz, A., Lo Iacono, C., Masqué, P., Palanques, A., Acosta, J., Guillén, J., Gómez Ballesteros, M., 2016a. Morphobathymetric analysis of the large fine-grained sediment waves over the Gulf of Valencia continental slope (NW Mediterranean). Geomorphology 253, 22–37.
Ribó, M., Puig, P., Urgeles, R., Van Rooij, D., Muñoz, A., 2016b. Spatio-temporal evolution of the sediment waves developed on the Gulf of Valencia margin (NW Mediterranean) during the Plio-Quaternary. Mar. Geol. 378, 276–291.
Ribó, M., Durán, R., Puig, P., Van Rooij, D., Guillén, J., 2017. Large sediment waves over the Gulf of Roses continental slope (NW Mediterranean). In: Guillén, J., Acosta, J., Chiocci, F., Palanques, A. (Eds.), Atlas of Bedforms in the Western Mediterranean. Springer, Cham.
Roca, E., Sans, M., Cabrera, L., Marzo, M., 1999. Oligocene to Middle Miocene evolution of the Central Catalan margin (northwestern Mediterranean). Tectonophysics 315, 209–233.
Sanchez-Cabeza, J.A., Masqué, P., Ani-Ragolta, I., 1998. ^{210}Pb and ^{210}Po analysis in sediments and soils by microwave acid digestion. J. Radioanal. Nucl. Chem. 227, 19–22.
Shapiro, G.I., Hill, A.E., 1997. Dynamics of dense water cascades at the shelf edge. J. Phys. Oceanogr. 27, 2381–2394.
Shapiro, G.I., Huthnance, J.M., Ivanov, V.V., 2003. Dense wáter cascading off the continental shelf. J. Geophys. Res. 108 (C12), 3390.
Sierro, F.J., Andersen, N., Bassetti, M.A., Berné, S., Canals, M., Curtis, J.H., Dennielou, B., Flores, J.A., Frigola, J., Gonzalez-Mora, B., Grimalt, J.O., Hodell, D.A., Jouet, G., Pérez-Folgado, M., Schneider, R., 2009. Phase relationship between sea level and abrupt climate change. Quat. Sci. Rev. 28, 2867–2881.
Stanley, D.J., Got, H., Kenyon, N.H., Monaco, A., Weilwe, Y., 1976. Catalonian, eastern Betic and Balearic margins: structural types and geologically recent foundering of the Western Mediterranean Basin. Smithson. Contrib. Earth Sci. 20, 67.
Tassone, A., Roca, E., Muñoz, J.A., Cabrera, L., Canals, M., 1996. Evolución del sector septentrional del margen continental catalán durante el Cenozoico. Acta Geol. Hisp. 29, 3–37.
Ulses, C., Estournel, C., Bonnin, J., Durrieu de Madron, X., Marsaleix, P., 2008a. Impact of storms and dense water cascading on shelf-slope exchanges in the Gulf of Lion (NW Mediterranean). J. Geophys. Res. 113, C02010.
Ulses, C., Estournel, C., Durrieu de Madron, X., Palanques, A., 2008b. Suspended sediment transport in the Gulf of Lions (NW Mediterranean): impact of extreme storms and floods. Cont. Shelf Res. 28, 2048–2070.
Ulses, C., Estournel, C., Puig, P., Durrieu de Madron, X., Marsaleix, P., 2008c. Dense shelf water cascading in the northwestern Mediterranean during the cold winter 2005: quantification of the export through the Gulf of Lion and the Catalan margin. Geophys. Res. Lett. 35, L07610.
Urgeles, R., Cattaneo, A., Puig, P., Liquete, C., De Mol, B., Amblàs, D., Sultan, N., Trincardi, F., 2011. A review of undulated sediment features on Mediterranean prodeltas: distinguishing sediment transport structures from sediment deformation. Mar. Geophys. Res. 32, 49–69.
Verdicchio, G., Trincardi, F., 2006. Short-distance variability in slope bed-forms along the Southwestern Adriatic Margin (Central Mediterranean). Mar. Geol. 234, 271–292.
Wilson, P.A., Roberts, H.H., 1995. Density cascading: off-shelf sediment transport, evidence and implications, Bahama banks. J. Sediment. Res. A65, 45–66.
Wynn, R.B., Stow, D.A.V., 2002. Classification and characterisation of deep-water sediment waves. Mar. Geol. 192, 7–22.
Wynn, R.B., Weaver, P.P.E., Ercilla, G., Stow, D.A.V., Masson, D.G., 2000. Sedimentary processes in the selvage sediment-wave field, NE Atlantic: new insights into the formation of sediment waves by turbidity currents. Sedimentology 47, 1181–1197.